

Towards a Diffraction-based Sensing Approach on Human Activity Recognition

FUSANG ZHANG, Peking University; Institute of Software, Chinese Academy of Sciences, China

KAI NIU, Peking University, China

JIE XIONG, University of Massachusetts, Amherst, USA

BEIHONG JIN, Institute of Software, Chinese Academy of Sciences; University of Chinese Academy of Sciences, China

TAO GU, Royal Melbourne Institute of Technology University, Australia

YUHANG JIANG, Peking University, China

DAQING ZHANG, Peking University, China

In recent years, wireless sensing has been exploited as a promising research direction for contactless human activity recognition. However, one major issue hindering the real deployment of these systems is that the signal variation patterns induced by the human activities with different devices and environmental settings are neither stable nor consistent, resulting in unstable system performance. The existing machine learning based methods usually take the “black box” approach and fails to achieve consistent performance. In this paper, we argue that a deep understanding of radio signal propagation in wireless sensing is needed, and it may be possible to develop a deterministic sensing model to make the signal variation patterns predictable.

With this intuition, in this paper we investigate: 1) how wireless signals are affected by human activities taking transceiver location and environment settings into consideration; 2) a new deterministic sensing approach to model the received signal variation patterns for different human activities; 3) a proof-of-concept prototype to demonstrate our approach and a case study to detect diverse activities. In particular, we propose a diffraction-based sensing model to quantitatively determine the signal change with respect to a target’s motions, which eventually links signal variation patterns with motions, and hence can be used to recognize human activities. Through our case study, we demonstrate that the diffraction-based sensing model is effective and robust in recognizing exercises and daily activities. In addition, we demonstrate that the proposed model improves the recognition accuracy of existing machine learning systems by above 10%.

CCS Concepts: • Human-centered computing → Ubiquitous and mobile computing systems and tools.

Additional Key Words and Phrases: Wireless sensing; Fresnel diffraction model; Human activity sensing; Wi-Fi

Authors’ addresses: F. Zhang, Key Laboratory of High Confidence Software Technologies (Ministry of Education), School of Electronics Engineering and Computer Science, Peking University; State Key Laboratory of Computer Sciences, Institute of Software, Chinese Academy of Sciences, Beijing, China; E-mail: zhangfusang@otcaix.iscas.ac.cn. K. Niu, Key Laboratory of High Confidence Software Technologies (Ministry of Education), School of Electronics Engineering and Computer Science, Peking University, Beijing, China; E-mail:xjtunk@pku.edu.cn. J. Xiong, College of Information and Computer Sciences, University of Massachusetts, Amherst, USA; E-mail:jxiong@cs.umass.edu. B. Jin, State Key Laboratory of Computer Sciences, Institute of Software, Chinese Academy of Sciences; University of Chinese Academy of Sciences, Beijing, China; E-mail:Beihong@iscas.ac.cn. T. Gu, School of Science, Royal Melbourne Institute of Technology University, Australia; E-mail:tao.gu@rmit.edu.au. Y. Jiang, School of Electronics Engineering and Computer Science, Peking University, Beijing, China; E-mail:1500012873@pku.edu.cn. D. Zhang, Key Laboratory of High Confidence Software Technologies (Ministry of Education), School of Electronics Engineering and Computer Science, Peking University, Beijing, China; E-mail:dqzhang@sei.pku.edu.cn. Corresponding Author: Daqing Zhang, Beihong Jin; E-mail:dqzhang@sei.pku.edu.cn, Beihong@iscas.ac.cn.

Permission to make digital or hard copies of all or part of this work for personal or classroom use is granted without fee provided that copies are not made or distributed for profit or commercial advantage and that copies bear this notice and the full citation on the first page. Copyrights for components of this work owned by others than ACM must be honored. Abstracting with credit is permitted. To copy otherwise, or republish, to post on servers or to redistribute to lists, requires prior specific permission and/or a fee. Request permissions from permissions@acm.org.

© 2019 Association for Computing Machinery.

2474-9567/2019/3-ART33 \$15.00

<https://doi.org/10.1145/3314420>

ACM Reference Format:

Fusang Zhang, Kai Niu, Jie Xiong, Beihong Jin, Tao Gu, Yuhang Jiang, and Daqing Zhang. 2019. Towards a Diffraction-based Sensing Approach on Human Activity Recognition. *Proc. ACM Interact. Mob. Wearable Ubiquitous Technol.* 3, 1, Article 33 (March 2019), 25 pages. <https://doi.org/10.1145/3314420>

1 INTRODUCTION

With the popularity of wireless devices and the ubiquitous deployment of Wi-Fi infrastructure, wireless sensing has attracted a lot of attentions in both academia and industry. Wireless sensing provides non-intrusive and continuous sensing over the air, opening a new direction to track user locations and sense their activities without attaching any device to a target. Adib et al. [4] and Pu et al. [32] firstly proposed to use Wi-Fi signal to recognize human activities. Subsequent works proposed to leverage Wi-Fi signal for fall detection [44] [39], gait recognition [41] and gesture classification [52],[14]. Utilizing Wi-Fi signal to extract motion information for interactive exergames and human exercise activity have been demonstrated in [31], [48] and [49]. The principle behind wireless sensing is that human activity affects the RF signal propagation, and different activities may cause different signal variation patterns. Each signal variation pattern may be associated to a particular activity, and hence Machine Learning (ML) method is typically applied to train a model for each signal variation pattern and infer the associated activity.

Although existing wireless sensing systems have achieved a success to some extent, many limitations exist. One big issue is that sensing performance is not always stable, and may fluctuate with respect to target location and transceiver position, limiting the real deployment of these systems. From benchmark experiments in our preliminary studies, we observe that while a target performs the same activity at the same location, the received radio signals may exhibit completely different variation patterns when the Wi-Fi receiver is placed at different locations in a room. On the other hand, when the target performs different activities, the received signals can be very similar with the same transceiver settings. These limitations pose a big challenge for RF-based activity sensing to be deployed in real world. Recent studies [37][55][47][56] reveal that radio signal propagation follows the theory of the Fresnel model which better explains the performance fluctuation of wireless sensing systems. However, there is a lack of quantitative studies to show how signal propagation is related to target location. This motivates us to investigate a deterministic sensing model, if possible, to quantify signal propagation with respect to target movement and better guide the system design and deployment.

The Fresnel zones consist of multiple concentric ellipses with two foci points on radio transmitter and receiver. Since radio propagation in the First Fresnel Zone (FFZ) (i.e., the innermost zone for the transceiver pair) has most obvious signal variations, we focus our study on the FFZ. Leveraging the Fresnel diffraction model [15][56], in this paper, we propose a diffraction-based sensing model to quantitatively determine the signal propagation with respect to a target's motions in the FFZ. The model eventually links the received signal variation patterns with motions, and hence can be used to detect human activities. We theoretically analyze our model, and conduct experimental measurements which prove our theoretical model. With this sensing model, we can thus guide the deployment of wireless sensing systems to significantly improve signal quality for activity detection. The study in this paper successfully breaks the sensing limit subjected by the “blindly” generated sensing signals in many existing sensing systems. Furthermore, the proposed model can be used to improve the performance of existing machine learning based sensing systems.

We develop a proof-of-concept prototype and apply the proposed sensing model to detect diverse activities (i.e., containing 7 body workout activities, walking and sitting) in the FFZ with a pair of Wi-Fi transceivers. Our model is able to accurately detect each activity, count the number of repetitive activities, and even tell the quality of workouts. Our model is orthogonal to the machine learning techniques and can be combined with them to further improve the recognition accuracy. The proposed sensing model can be applied to recognize a large variety of motion activities. The main contributions are summarized as follows.

- This work investigates a diffraction-based sensing model to explain the reason behind the performance instability which is a major issue for existing sensing system. This work sheds light on a new deterministic approach for wireless activity sensing.
- We analyze the signal propagations with respect to target location in the FFZ, and develop a mathematical model to establish the quantitative relationship between the signal variation and target location. We verify this model through benchmarking experiments and reveal several important properties for target sensing.
- Based on the proposed sensing model, we build a proof-of-concept system for detecting repetitive motion activities. We employ the unique signal variation induced by each activity to recognize the activity. Our experiments demonstrate that the system is effective and robust against ambient environmental changes. In addition, the proposed model improves the recognition accuracy of machine learning systems by above 10%.

2 PRELIMINARY STUDY

In this section, we conduct our empirical studies on wireless sensing based activity recognition using machine learning methods. We use commodity Wi-Fi devices, and take repetitive motion activities (i.e., body workouts) as an example. We evaluate five feature-based learning methods and an advanced neural network method with three manually collected human exercise data sets. Finally, we compare the results of these methods and present our observations which reveal the issues in existing methods.

2.1 Experimental Setup

We take 3 commonly seen workout activities as examples, i.e., sit-up, push-up and walkout. According to the existing study of human activity sensing [39], human activities can be performed on Line-of-Sight (LoS) and Non-Line-of-Sight (NLoS) of the transceiver pair to be sensed. The study in [39] shows that the amplitude variation caused by human activity becomes much weaker when the target is not located at the LoS. This is because more than 70% of the energy is transferred via the zone near to LoS [16]. In this experiment, the exercise mat is thus placed between the transceivers and the target performs activities on the mat. We select three different placements of the Wi-Fi transceivers in a typical indoor environment and the transceivers are placed at the same height from 0 to 40 cm at a step size of 20 cm. For each equipment setting, eleven volunteers are asked to perform 3 activities with 5 repetitions. We obtain a total of 495 ($3 \times 11 \times 3 \times 5$) workout activities. We collect the amplitude of the Channel State Information (CSI) from the Wi-Fi receiver. The signal amplitude can be seen as a time series sequence $x = (x_1, x_2, \dots, x_n)$. If there is no moving target in the environment, the wireless channel is relatively stable. When the target performs activity, the scattered signal from the target changes, which results in obvious signal variations. *Human activity can be recognized by mapping different signal variation patterns to corresponding human activities.*

2.2 Activity Recognition with Classical Methods

Following the classical learning based methods [53][39], we normalize the signal, segment each cycle of the repetitive activity and label the sensing signal with corresponding activity. In order to recognize the activities, we extract the following features from the CSI amplitude sequences:

- 1) the mean and standard deviation of CSI, which are given by $\mu = \frac{1}{|x|} \sum_{i=1}^{|x|} x_i$ and $\delta = \sqrt{\frac{\sum_{i=1}^{|x|} (x_i - \mu)^2}{|x|}}$;
- 2) the maximum and minimum value of x ;
- 3) the skewness ($Skew(x) = \frac{E(x-\mu)^3}{\delta^3}$);
- 4) the kurtosis ($Kurtosis(x) = \frac{E(x-\mu)^4}{\delta^4}$);

Table 1. Activity recognition accuracy

| Classification Method | Accuracy (495 activities) | Accuracy (990 activities) | Accuracy (1980 activities) |
|----------------------------|------------------------------|------------------------------|-------------------------------|
| Gaussian Kernel SVM | 0.65 | 0.68 | 0.66 |
| Decision Tree (DT) | 0.66 | 0.66 | 0.68 |
| K-Nearest Neighbors (KNN) | 0.67 | 0.69 | 0.67 |
| Random Forest (RF) | 0.71 | 0.72 | 0.73 |
| Discriminant Analysis (DA) | 0.53 | 0.64 | 0.63 |
| CNN | 0.81 | 0.82 | 0.82 |

5) root sum square $\theta = \sqrt{\sum_{i=1}^{|x|} x^2}$ and
6) the q-quantiles ($q=0.25, 0.5, 0.75$).

Based on the above 10 ($2+2+1+1+1+3$) features extracted from the received signal, we apply 5 different classification methods including Support Vector Machine (SVM), Decision Trees (DT), K-Nearest Neighbors (KNN), Random Forest (RF) and Discriminant Analysis (DA) to identify the activities. The recognition accuracies are shown in Table 1. We observe that Random Forest achieves the highest accuracy of 71%.

Typically, a larger training set may improve recognition accuracy. Thus we collect another two groups of datasets for 11 targets performing the three workout activities when the transceivers are placed at a height from 0 cm to 50 cm at a step size of 5 cm and 10 cm, respectively. The other two datasets contain 990 ($6 \times 11 \times 3 \times 5$) and 1980 ($12 \times 11 \times 3 \times 5$) activities. As shown in Table 1, some of the classification methods indeed have small performance improvement. However, we also notice that increasing the size of the dataset does not always help. Besides, the misclassification rates are quite high, ranging from 27% to 37%, which hinders in building any practical applications.

Another possible reason for the poor performance is that the extracted features may not be able to fully describe the uniqueness of the signal change caused by each activity. We thus apply the advanced Convolutional Neural Network (CNN) method which can automatically extract informative features on the same data set. We design a CNN-based neural network consisting of six layers. The framework of our neural network structure is shown in Fig. 1. The CSI amplitude values are the input data. During the training process, the input data are resized to a 1×64 vector. We use three convolutional layers for extracting features from the Wi-Fi CSI data. For the three convolutional layers, the sizes of the filters are all set to 5. The number of the filters on each convolutional layer is set to 60. For the pooling layers, we use the max pooling. The pooling size is set to 2. All the activation functions are ReLU ($\text{ReLU}(x)=\max(0,x)$). After feature extraction in the convolutional layers, we use two fully connected layers. To make the neural network generalize well in practice, we use dropout to reduce overfitting. The dropout rate for CNN is set to 0.5. At last, we employ a softmax Loss function [25] as the classifier for the output of the neural network. We adopt the learning rate decay method and train 500 epochs in total. The proposed learning model is implemented using Pytorch [3]. As shown in Table 1, the CNN-based method achieves the highest recognition accuracy while the improvement with larger dataset is very limited. We finally achieve an average accuracy of 82%.



Fig. 1. Neural network in the CSI-based activity recognition system

2.3 Result Analysis

We ask the question why the advanced ML method with a large dataset is still not able to achieve a high accuracy¹?

Assumption 1: Each activity corresponds to a stable and consistent signal variation pattern.

Counter observation: Take sit-up activity as an example. As shown in Fig. 2, the sensing signal of the same activity exhibits totally different variations when the transceivers are placed at different locations. Fig. 2a shows only one valley while Figs. 2b-2d have two or more valleys.

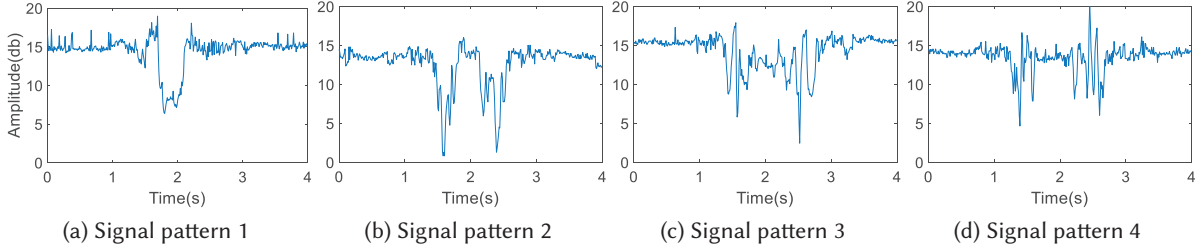


Fig. 2. Observation 1: different signal patterns for the same sit-up activity.

Assumption 2: Different activities correspond to different signal variation patterns.

Counter observation: When the target performs different activities, e.g., sit-up and push-up, we notice that the sensing signal can be very similar. As shown in Fig. 3a and Fig. 3b, with specific equipment deployment, the sensing signals are almost the same. Fig. 3c and Fig. 3d show another two signal variations which are very similar but are induced by different activities.

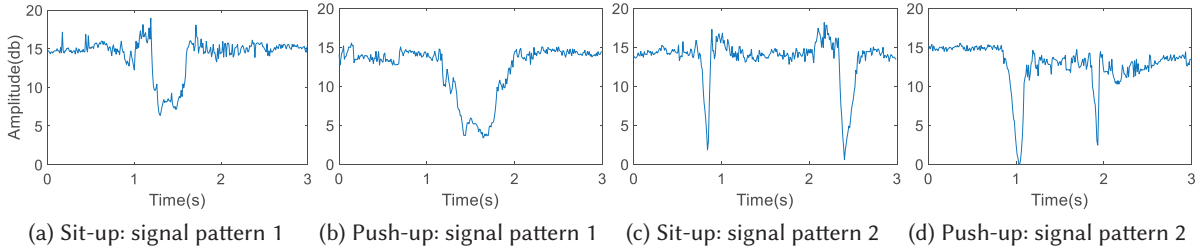


Fig. 3. Observation 2: similar signal patterns resulting from the sit-up and push-up activities.

These two counter observations show that arbitrary sensing setting breaks the assumption of one-to-one mapping between activity and signal variation pattern. The learning based methods thus have inherent difficulties to address the ambiguities brought in. Furthermore, the existing sensing techniques have cognitive gaps in understanding the uncertainty and indistinguishable signal patterns induced by human activities, which also pose a big challenge to achieve reliable sensing performance. We argue that a method to establish the quantitative relationship between target's location, equipment placement and signal variation patterns is needed. We thus revisit this issue with the Fresnel diffraction model to fundamentally understand how human motions affect signal propagation and signal variations at receiver.

¹We consider higher than 90% as high accuracy.

3 DIFFRACTION-BASED SENSING MODEL

In this section, we first provide the background of the basic Fresnel Zone model. We focus our study on the First Fresnel Zone (FFZ) where signal propagation follows the diffraction theory. We then propose our diffraction-based sensing model which quantitatively models signal strength for repetitive motion activities. We analyze this model theoretically, and prove it through a series of measurement experiments.

3.1 The Basics of Fresnel Model

Consider a free-space scenario, the transmitter Tx transmits RF signals with a wavelength of λ to the receiver Rx . The Fresnel zones are concentric ellipses with foci of transmitter and receiver as shown in Fig. 4. The boundary of the n th Fresnel zone is defined as

$$|TxP_n| + |RxP_n| - |TxRx| = n\lambda/2 \quad (1)$$

where P_n is a point on the n th ellipse [37]. The innermost ellipse ($n=1$) is defined as the First Fresnel Zone (FFZ). Let O be a point on LoS between two transceivers, the length of TxO and RxO is d_1 and d_2 , respectively. The radius of FFZ can be calculated as $r_1 = \sqrt{\frac{\lambda d_1 d_2}{d_1 + d_2}}$. When $d_1 = d_2$, the r_1 is $\sqrt{\frac{\lambda d}{2}}$ ($d = d_1 = d_2$).

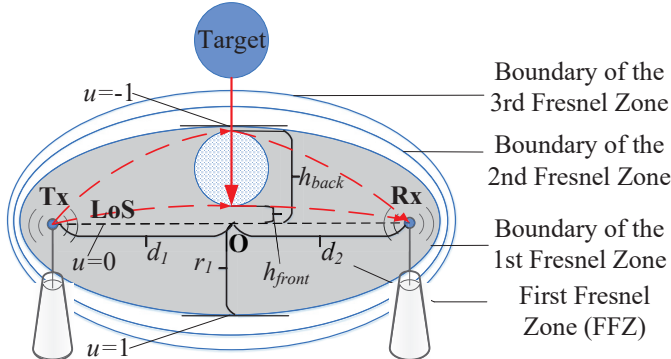


Fig. 4. Diffraction effects in the First Fresnel Zone.

Studies [16] show that between a pair of Wi-Fi transceivers more than 70% of RF signal energy is transferred via the First Fresnel Zone. When a target moves into the First Fresnel Zone, diffraction becomes much stronger and dominates, which means the target blocks the primary energy pathway and the remaining energy bypass the target. When applied to activity sensing, this may imply strong signal variations to different activities, potentially achieving better sensing performance.

3.2 Diffraction-based Sensing Model

We now investigate the scenario when a human target is inside the FFZ. We are interested in finding out how signal propagation is affected when the target moves back and forth in the FFZ. The size of the FFZ is determined by an ellipse originated at the middle point of the Line of Sight (LoS). The horizontal axis lies on the LoS of the transceiver pair, and the vertical radius is defined as r_1 . We set the vertical axis with an upper boundary $u_{front} = -1$, and a lower boundary $u_{back} = 1$. We use the full cylinder model to represent the complete human body. We consider the scenario where a target moves back and forth along the vertical axis. The diffracted signals propagate from Tx to Rx, bypassing the cylinder, as shown in Fig. 4. To indicate the position of a target, we define h_{front} and h_{back} as the distances from the front and back side of the target to the LoS of the transceivers, as

shown in Fig. 4. We then normalize these two distances as *Fresnel front clearance* $u_{front} = \frac{h_{front}}{r_1}$ and *Fresnel back clearance* $u_{back} = \frac{h_{back}}{r_1}$. When the front edge touches the LoS, $h_{front} = 0$ and $u_{front} = 0$. When the front edge first touches the upper boundary of the FFZ, we have $h_{front} = -r_1$ and $u_{front} = -1$. When the front edge moves further and reaches the lower boundary, we have $h_{front} = r_1$ and $u_{front} = 1$. Then the Fresnel-Kirchhoff diffraction parameter v_{front} can be expressed by Fresnel clearance u_{front} as

$$v_{front} = h_{front} \sqrt{\frac{2(d_1 + d_2)}{\lambda d_1 d_2}} = h_{front} \frac{\sqrt{2}}{r_1} = \sqrt{2} u_{front} \quad (2)$$

Thus, the signal amplitude at the receiver due to front side diffraction describes the integral of received signals diffracted from the front side of the target to infinity, which is given as follows.

$$F(v_{front}) = \frac{1+j}{2} \cdot \int_{v_{front}}^{\infty} \exp\left(\frac{-j\pi z^2}{2}\right) dz \quad (3)$$

Where the $\exp\left(\frac{-j\pi z^2}{2}\right)$ is the phase shift for a diffraction path z . Integration with respect to z from v_{front} to positive infinity cumulates all the signal path diffracted from the front side of target. Similarly, the back side diffraction describes the integral of received signals diffracted from negative infinity to the back side of the target. We integrate over z from negative infinity to v_{back} to cumulate the path diffracted from the back side of target, which is given as follows.

$$F(v_{back}) = \frac{1+j}{2} \cdot \int_{-\infty}^{v_{back}} \exp\left(\frac{-j\pi z^2}{2}\right) dz \quad (4)$$

In summary, the total diffraction gain due to the presence of a target inside the FFZ is thus given by adding the gains of both sides

$$Gain_{Diff} = 20\log|F(v_{front}) + F(v_{back})| \quad (5)$$

3.3 Signal Amplitude Variation When Target Moves Inside the FFZ

In this section, we first utilize the Fresnel diffraction model to present the theoretical analysis of the signal amplitude variation when the target moves into the Fresnel zones. We then verify the theoretical results with our testbed experiments.

3.3.1 Theoretical Analysis. To understand the effect on the received signal during the process when a target moves into the FFZ, we model human body as a circular cylinder. We try two different size cylinders with a diameter of 20 cm and 30 cm, respectively. The distance between the two Wi-Fi transceivers is set to 2 m. With a 2 m LoS distance, the radius of FFZ is 17 cm. We simulate the process of the cylinder's move starting from the position -51 cm (measured from the center of gravity) away from the LoS, corresponding to a Fresnel front clearance (u_{front}) of -2.4 (-51+10=-41 cm) and -2.12 (-51+15=-36 cm) for the two cylinders, respectively. The cylinder stops at 3 different positions, shown in Fig. 5 (top): 1) when the front edge of the cylinder touches the LoS ($u_{front}=0$); 2) when the front edge reaches 34 cm ($u_{front}=2$); and 3) when the front edge reaches 51cm ($u_{front}=3$). By calculating both the Fresnel front and back diffraction with Eq. 5, the received signal amplitude during the whole process is plotted in Fig. 5 (bottom). The signal amplitude is symmetric with the center of the cylinder located at the LoS.

If we consider a repetitive movement in which the target moves to a position, stops and then moves back to the original position, the amplitude of the signal during the process exhibits symmetry with respect to the stopping position. Fig. 6 shows the signal amplitude of the repetitive movements with 3 different stopping positions. We can observe three unique patterns with different stopping positions. When the target stops at $u_{front} = 0$ in

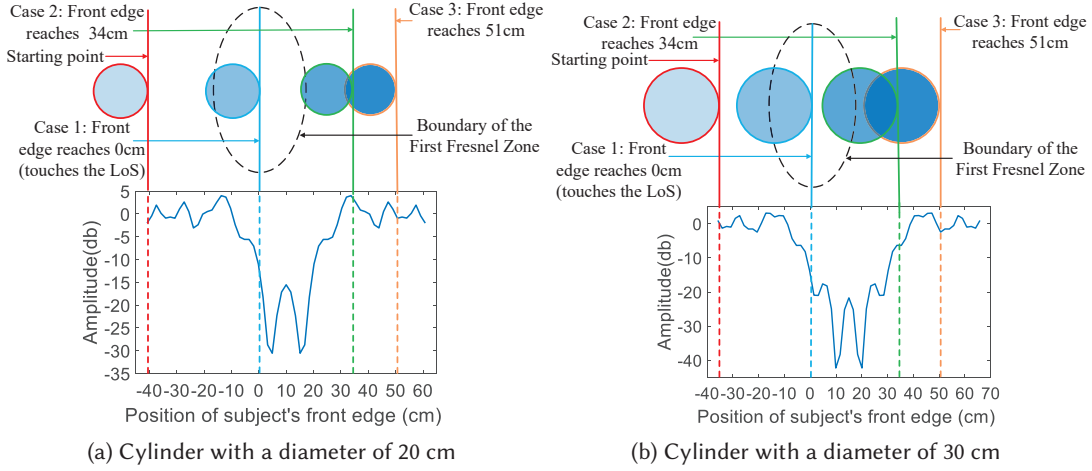


Fig. 5. Signal changes with target moving.

Fig. 6a, we observe a clear single valley. When the target stops at $u_{front} = 2$ and $u_{front} = 3$, we can observe four valleys in Fig. 6b and Fig. 6c, respectively. The distance between the middle two valleys increases when the target stops at a further position inside the FFZ after the target crosses over the LoS. In Fig. 7, we show the results when the diameter of the cylinder becomes 30 cm. We can see that although there are slight changes, the overall patterns are still very similar to those generated with a 20 cm diameter cylinder. This property guarantees the robustness against different human target sizes when we apply the signal amplitude patterns for activity sensing. We summarize the properties which can be utilized for repetitive activity sensing in Section 3.4.

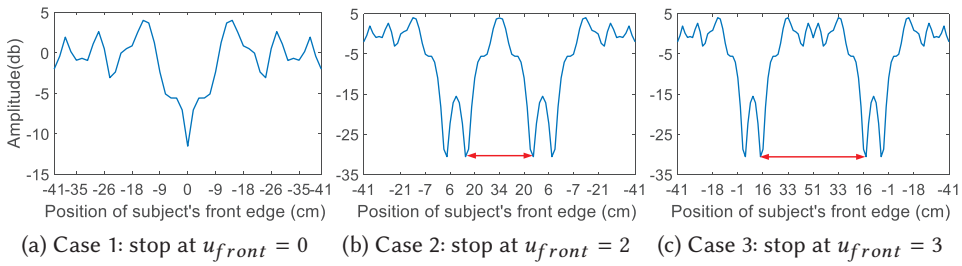


Fig. 6. The cylinder with a diameter of 20cm moves inside the FFZ with repetitive motions.

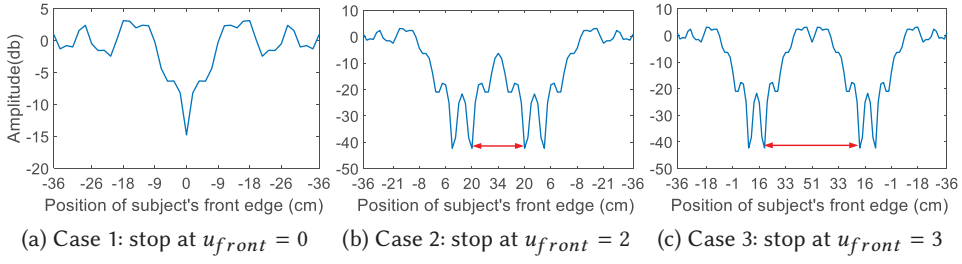


Fig. 7. The cylinder with a diameter of 30cm moves inside the FFZ with repetitive motions.

3.3.2 Verification with Benchmark Experiments. We verify the Fresnel diffraction model proposed in previous section with experiments. The experimental setup is shown in Fig. 8. The two Wi-Fi transceivers are placed 2 m apart. We employ two different size cylinders as the targets which have a diameter of 20 cm and 30 cm, respectively. The heights of cylinders are 20 cm. To generalize model verification for human size object, we utilize a model of human body with chest width 20 cm to simulate the human repetitive activity. The cylinders and human body model move into the FFZ repetitively with the help of a sliding track. We set the speed of the sliding track as 13 cm/s. The antennas at the two transceivers are placed at the same height. The sliding track is aligned to the perpendicular bisector of the transceiver pair. The central carrier frequency is 5.24 GHz and the signal wavelength is 5.7 cm.

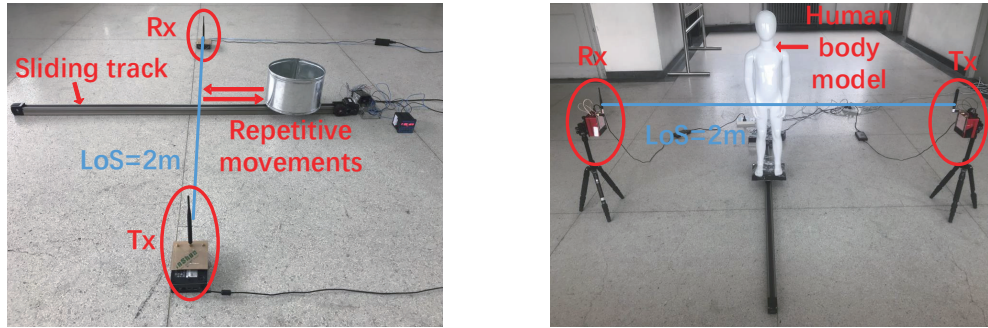


Fig. 8. The experimental environment and deployment of transceivers.

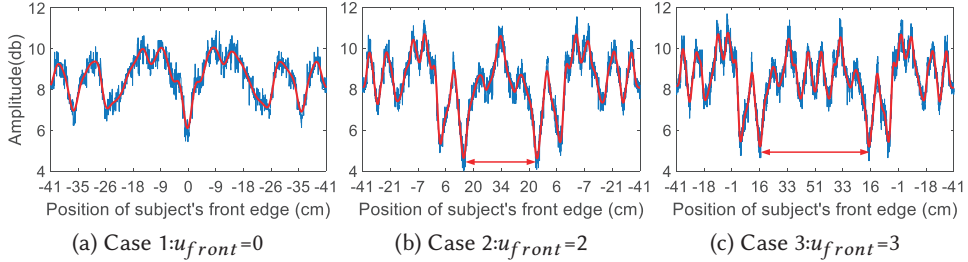


Fig. 9. The signal variation due to the movement of a 20cm cylinder with Intel 5300 Wi-Fi card.

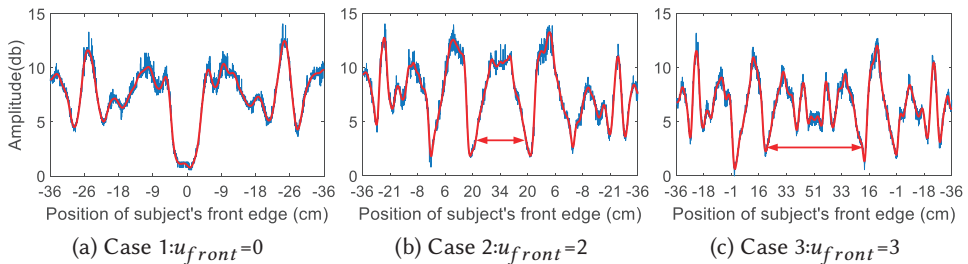


Fig. 10. The signal variation due to the movement of the human body model with Intel 5300 Wi-Fi card.

We present the experimental results for the 20 cm cylinder with commodity Wi-Fi devices in Fig. 9. The target starts at the position -41 cm away from the LoS and stops when the front side crosses over the LoS by 0 cm, 34 cm and 51 cm, respectively. The target then returns back to the starting point and complete a full cycle of movement. Fig. 9 shows the signal amplitude of one movement cycle for the three stopping positions. The red

lines are the smoothed signals², while the blue lines are the raw signals. We can see that the real-life experimental results match the theoretical plots in Fig. 6 very well. For case 1, only one valley appears as we expect. For case 2 and case 3, four valleys are clearly observed. More importantly, the first two valleys are separated from the second two valleys with a larger distance when the cylinder moves across LoS further inside, exactly matching the theoretical plots in Fig. 6b and Fig. 6c. The results of the larger 30 cm cylinder also match the theoretical plots well and we skip them here. Fig. 10 shows the experimental results for human body model performing one movement cycle inside the FFZ. The experimental results also match the theoretical plots well.

Note that we only use amplitude but not phase because the raw phases provided by commodity WiFi cards are random, which cannot be directly used. We agree that the accurate phase information can be used for activity recognition. With software-defined radio platform such as WARP, we can obtain both correct amplitude and phase information to recognize activities. In the future work, we plan to utilize the amplitude and phase difference across multiple antennas obtained from the same WiFi card to further improve the recognition accuracy.

3.4 Key Properties Obtained for Repetitive Motion Sensing

With both theoretical analysis and benchmark experiments, we summarize the unique diffraction-related properties in the FFZ which can be utilized for repetitive activity sensing as follows:

- (1) When the target enters into the FFZ, the signal amplitude experiences an obvious descent process. This leads to a unique and non-monotonous signal pattern which forms the basis of activity sensing.
- (2) For a complete cycle of a repetitive movement, the signal amplitude exhibits a clear symmetry with respect to the stopping positions.
- (3) For a repetitive movement, when the target stops at different locations inside the FFZ, we observe different signal patterns. If the stopping positions are before the LoS, one single valley is observed. After the target crosses over the LoS, we observe multiple valleys. If the target moves further, the spacing between the valleys increases accordingly.

4 GUIDING SYSTEM DESIGN FOR REPETITIVE ACTIVITIES

In this section, we design a sensing system for repetitive activity recognition leveraging on our proposed model in Section 3. Based on the diffraction-related properties, our model is able to guide the system to obtain an optimized equipment deployment, which generates the differentiable signal patterns for different activities on purpose. Without loss of generality, we use workout activities (i.e., sit-up and push-up) as examples to illustrate the principle.

4.1 System Overview

Our sensing system can assist users to understand their repetitive activity status, including activity types, activity duration, number of repetitions and whether the activities are in proper forms. The users can utilize the detailed statistics to achieve more effective workouts.

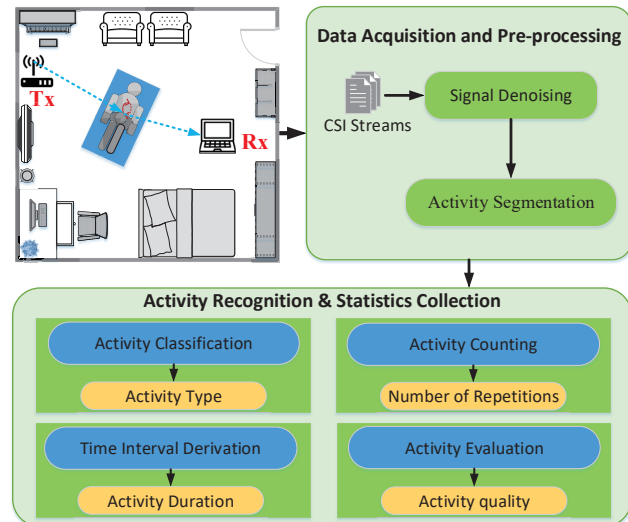


Fig. 11. System overview.

²We present the denoising method in Section 4.2.

As illustrated in Fig. 11, our system works in two stages: (1) data acquisition and pre-processing; (2) activity recognition and statistics collection. In data acquisition and pre-processing stage, raw Channel State Information (CSI) readings from commodity Wi-Fi receivers are taken as input. The raw signals are usually noisy. So we apply carefully designed filters to smooth out the random noise. Activity recognition and statistics collection are the core parts of our system, which contains four modules: activity classification, repetition time interval derivation, activity counting and activity quality evaluation. Activity classification module identifies the individual exercise activity. Repetition time interval derivation module determines the starting time and ending time of each single activity cycle and calculates the interval accordingly. Activity counting module counts the number of repetitions. The evaluation module assesses if the activities are performed in proper forms.

4.2 Data Acquisition and Pre-processing

To identify a repetitive activity, we start the process by collecting raw CSI readings from the commodity Wi-Fi devices. The raw signals induced by 3 cycles of sit-up activities are noisy as shown in Fig. 12. To obtain accurate amplitude variations for segmenting each activity, it is necessary to denoise the raw signal. We remove the small random variations and still reserve the large signal variation caused by activity movement. We adopt the Savitzky-Golay filter to process the raw signal. Savitzky-Golay filter (also known as least-square smoothing filter) fits successive subset of adjacent data points with a low degree polynomial by the method of linear least square [36]. After the filter is applied, the raw signal gets smoothed as red lines in Fig. 13. We originally have four valleys within one cycle in the raw signal. As each two of them has a fixed small spacing, they are merged into two valleys after filtering. Hence, we can observe two obvious valleys in each activity cycle after filtering.

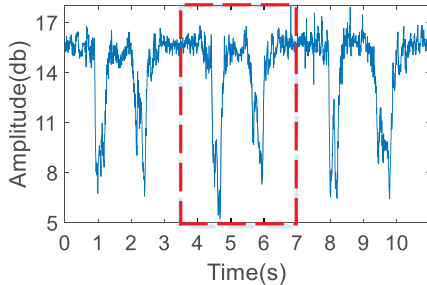


Fig. 12. The raw CSI amplitudes collected from Wi-Fi devices.

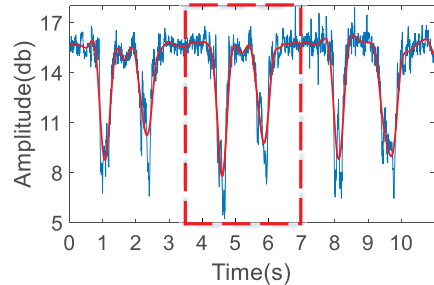


Fig. 13. The denoised CSI amplitudes with Savitzky-Golay filter.

4.3 Model Guides System Deployment and Activity Classification

In this section, we investigate how to guide the system deployment by Fresnel diffraction model. We use sit-up and push-up as examples to demonstrate how we generate easily distinguishable signal patterns for each activity. The intuition is that sit-up has a larger movement distance than push-up³. Based on the sensing properties, we know that when the target stops at different positions inside the FFZ, we can obtain different signal amplitude patterns (i.e., different number of valleys). Inspired by this observation, we can place the transceivers at a chosen height, which makes the two activities have clear different stopping positions inside the FFZ. Consequently, we can observe obvious amplitude pattern difference during the process of sit-up and push-up. Besides, our system can also accurately identify other workout activities as shown in Section 5.

³The movement distance of push-up is around 20cm while sit-up is around 60cm.

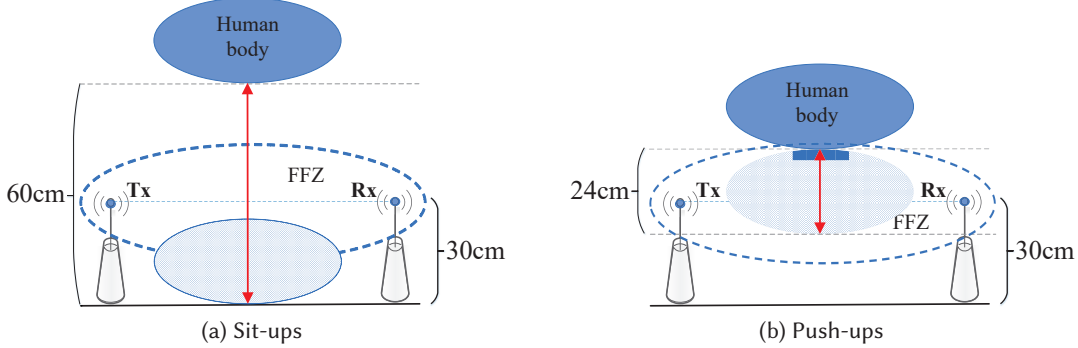


Fig. 14. Experimental setup.

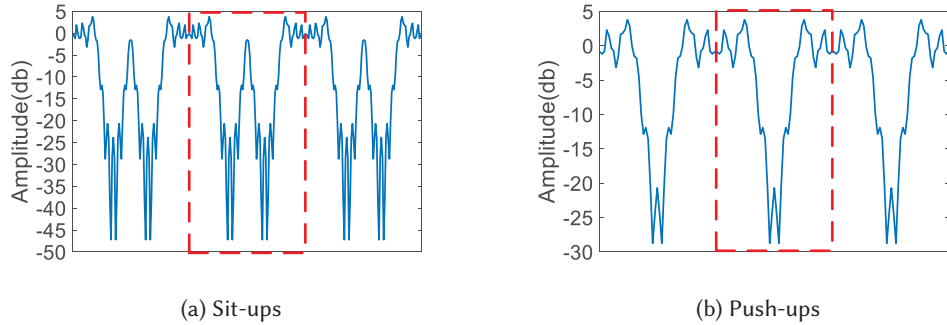


Fig. 15. Theoretical plots of signal amplitude variations for sit-up and push-up activities.

We employ the deployment shown in Fig. 14 as an example. The height of the antennas is set as 30cm. The body thickness of the exerciser is 24cm. When performing sit-ups, the exerciser starts from a height of 60cm (measured from the exerciser's shoulder) and moves until the back touches the ground. From the Fresnel diffraction model perspective, the moving range is from $[u_{front}, u_{back}] = [-1.76, -3.17]$ to $[u_{front}, u_{back}] = [1.76, 0.35]$. While performing push-ups, the movement distance of the exerciser is 24cm. Thus, the sit-up movement crosses the entire FFZ, which leads to a total of four valleys. Note that the two valleys close to each other may get merged when there is noise. To remove possible ambiguities, we deliberately apply a filter to merge the two close-by valleys into one. We calculate the received signal variation pattern using diffraction model in Section 3.1, and plot the theoretical result in Fig. 15a. On the other hand, for push-up, the target only enters half of the FFZ. Thus only two valleys can be observed as shown as in Fig. 15b. We also deliberately apply a filter to merge the two close-by valleys into one to remove the ambiguities caused by noise. The unique signal patterns make it possible for us to distinguish the two activities. With these signal patterns, we are able to apply the CNN-based learning network to easily differentiate different human activities. The real-life experimental results with human target are presented in Section 5.2.

4.4 Repetition Time Interval Derivation

Our system can derive the time interval of one complete cycle of an activity which indicates the speed of each activity. For sit-up, the exerciser starts from sitting and moves to lying down (stops) and then gets up back to sitting again.

To acquire the starting and ending points of an activity, we find the variance of CSI amplitude is very sensitive to target's movements. It is observed that when there are no movements, the signal variation is quite small. The average variance is below 0.2. On the other hand, when there are human activities inside the FFZ, we observe much larger CSI amplitude fluctuations and the average variance increases to 2, which is 10 times larger. So the state transition of the CSI amplitude variance is utilized as the parameter to identify the starting and ending points of the activity. We utilize a 0.2s sliding window (40 samples) with a 50% overlay to estimate the amplitude variance. The maximum variance when there are no activity movements is chosen as the threshold to detect movements. Fig.16 (up) shows the raw signal amplitudes and Fig.16 (bottom) shows the calculated signal variance for three activity cycles. The horizontal solid red line is the variance threshold. The starting and ending points of an activity can be clearly identified. With this information, we can extract the repetition time interval and number of activities as shown in Fig. 16.

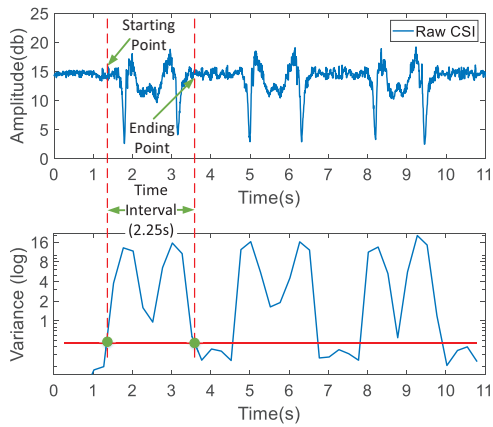


Fig. 16. Obtaining the starting and ending time points for the time interval of each activity.

4.5 Assess if the Activities are Performed in Proper Forms

In this section, we show that our system can further assess the quality of the activity (whether the activity is performed properly). Our system can check if the chest is lowered down enough for push-up and if the back is placed to the ground before moving back to the origin for sit-up.

Taking sit-up as the example for illustration. With the same deployment setup in Section 4.3, the exerciser performs some non-standard sit-ups. The start position of the activity is the same, but the exerciser does not move his back to touch the ground. As shown in Fig. 17, we consider three cases: i) the body moves slightly by 25 degrees (i.e., the back touches the boundary of the FFZ, $u_{front} = -1$, $u_{back} = -2.41$); ii) the body moves by 60 degrees (i.e., the back touches the LoS, $u_{front} = 0$, $u_{back} = -1.41$) and iii) the body moves close to the ground by 75 degrees (i.e., the back touches the other side of the FFZ boundary, $u_{front} = 0.8$, $u_{back} = -0.61$). Fig. 17 shows the theoretical signal patterns during the process of the three “non-standard” sit-ups. They are quite different from the signal pattern obtained in a “standard sit-up”. As shown in Fig.17 (d-f), for the former two cases, the signal patterns are significantly different from the pattern obtained from a standard sit-up. For case 3, we observe the same number of valleys but with a much smaller spacing. This spacing between the two valleys can be used as a metric to assess if a sit-up is performed properly. For push-up, we assess if the activity is in a proper form by checking the amplitude change range during the process. The experimental results are presented in Section 5.4.

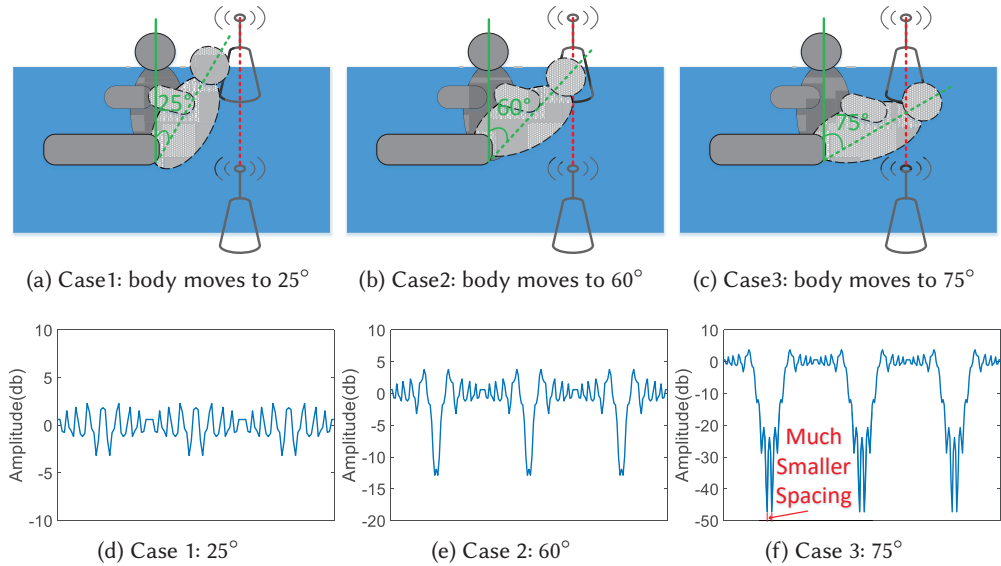


Fig. 17. The experimental setup and the theoretical results for three different improper sit-ups.

4.6 Recognizing Daily Activities with Fresnel Diffraction and Reflection Models

Besides recognizing repetitive activities in the FFZ, the Fresnel diffraction model can be combined with Fresnel reflection model [37][47] to recognize daily activities accurately in a much larger sensing range. While the target subject performs activities in the FFZ, the Fresnel diffraction model is employed to understand the received signal variation patterns and guide the system design, while the subject performs activities outside the FFZ, the Fresnel reflection model can be applied. In this way, either repetitive activities in the FFZ or other daily activities outside the FFZ can be well recognized with the Fresnel models.

5 EVALUATION

To evaluate the performance of the proposed diffraction-based sensing model, we implement a proof-of-concept prototype to detect repetitive activities using commodity Wi-Fi devices in the FFZ. We conduct comprehensive experiments to demonstrate the effectiveness of the proposed sensing model. With the model guidance, we present the activity classification accuracy, the counting accuracy, the repetition time interval derivation, and access if the activities are in proper form. Then we show the system performance when more human daily activities are performed in three living environments with much larger sensing range. Finally, we evaluate the effect of interference movement from surrounding people.

5.1 Experimental Setup

Setup 1: Our prototype system consists of one Wi-Fi transceiver pair. Each transceiver is a Gigabyte mini-PC equipped with a cheap Intel 5300 Wi-Fi card. The receiver is equipped with three antennas running on the 5.24 GHz channel. We collect the CSI readings from the Wi-Fi card with the CSI-tool [12]. Taking the CSI readings as input, we process the raw readings using Savitzky-Golay filter. The packet transmission rate is 200 packets per second. We choose and place the equipments as the Fresnel diffraction model guided previously. We build a

web-based user interface to show the activities detected in real-time in Fig. 18. The demo video is provided at link: <https://youtu.be/I0BDK53djhg>.

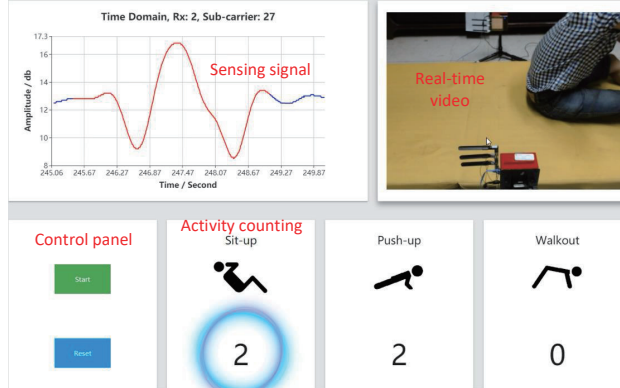


Fig. 18. Real-time system user interface.

Setup 2: To support Wi-Fi based sensing in realistic scenarios, we also employ Intel 7265 Wi-Fi card⁴ to evaluate the performance of our system in multiple realistic scenarios (e.g., real home and office environment). The existing Wi-Fi infrastructure such as a TP-link access point shown in Fig. 19a can directly communicate with a Wi-Fi device equipped with this card and thus allow us to obtain the CSI for sensing. Intel is planning to support exporting CSI on more Wi-Fi cards in the near future and we believe more and more commodity Wi-Fi devices can be employed for sensing. We do not require any dedicated Wi-Fi packet transmission for sensing. The current 802.11 Wi-Fi standard requests the AP to periodically ping the Wi-Fi device connected and these ping packets sent out every 0.1s are enough for us to perform sensing. This ensures that our sensing task does not require dedicated packet transmission and thus does not interrupt the ongoing data communication. Considering a home/office environment with one Wi-Fi access point in the corner (in Fig. 19c), any Wi-Fi link between this AP and a Wi-Fi-capable device (e.g., phone, tablet, miniPC, or laptop in Fig. 19b) can then be utilized for sensing. We conduct experiments to recognize activities under three practical scenarios in Sections 5.6-5.8.



Fig. 19. Wi-Fi devices and scenario

⁴We signed an agreement with Intel Corporate Research Council/ University Research Office (URO) and they provide us full access to Intel 7265 802.11n Wi-Fi card to extract CSI for contactless Wi-Fi sensing.

5.2 Overall Performance

In this section, we conduct experiments to evaluate the overall performance of our activity recognition system. We demonstrate our system can sense and differentiate different repetitive activities, e.g., push-up, sit-up and walkout. Fig. 20 illustrates the schematic of these exercises.

We ask the volunteers to perform these exercises and Fig. 20 (d-f) show the signal amplitude changes during the process. We can observe clear differences between these activities. For push-up, the signal has one obvious valley. Sit-up and walkout have a larger scale of movement and thus cause two valleys and more. These unique signal patterns guided by our model remove the possible ambiguities and guarantee the stable performance in identifying each activity.

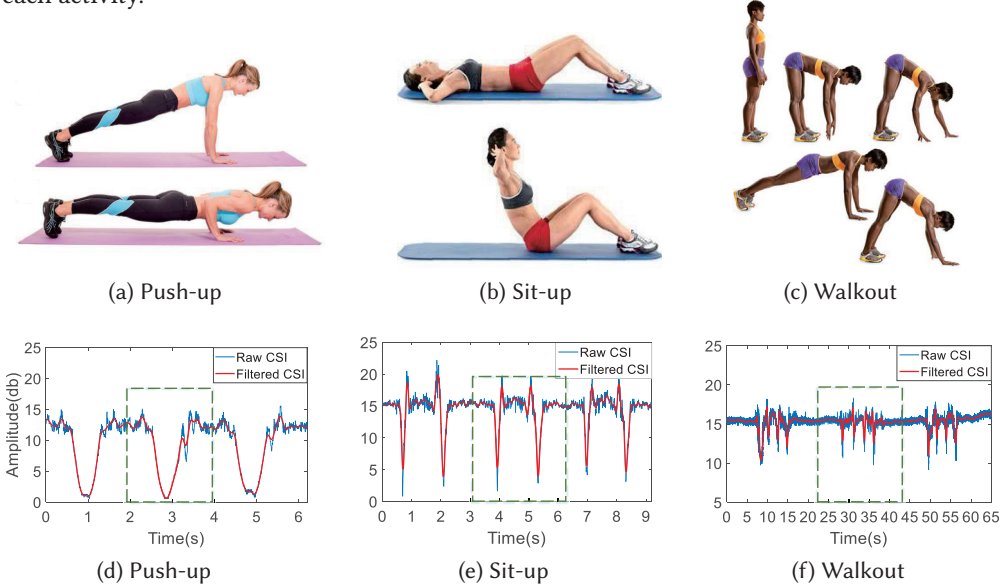


Fig. 20. The signal amplitude patterns for 3 exercise activities.

We recruit eleven volunteers including two female and nine male students to perform exercise activities in rooms of different sizes for performance evaluation. We ask the volunteers to perform 66 groups of each activity with 5 repetitions in each group. We classify these activities using the proposed Convolutional Neural Network (CNN) method in Section 2. As shown in Fig. 21, on average, our diffraction model based method can improve both precision and recall for activity recognition to 95% above, compared with 82% for CNN method without model guidance.

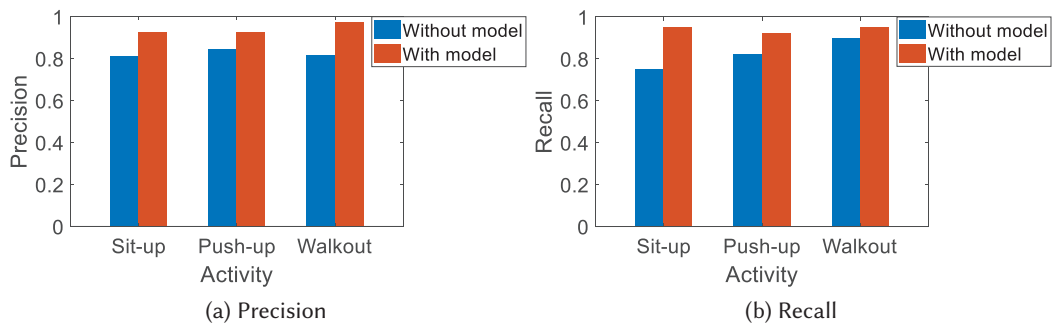


Fig. 21. Performance comparison between without the model guidance and with the model guidance.

5.3 Measuring the Time Interval of Each Activity

We can derive the time interval of each repetition during the whole activity process. The system can know whether the intensity level is proper and suggest the exerciser to adjust the rhythm of the exercise accordingly. We ask the volunteers to perform sit-ups with different speeds, respectively. Fig. 22 shows the signal amplitude when a volunteer performs sit-ups at a fast and a slow speed, respectively. The duration of each sit-up cycle is annotated in the figure. The time interval is 1.75 seconds for fast sit-ups and 2.75 seconds for slow sit-ups. We believe this fine-grained real-time⁵ information can be used as an instantaneous feedback to the user to adjust the speed and is also useful in analyzing the whole repetitive activity process later offline.

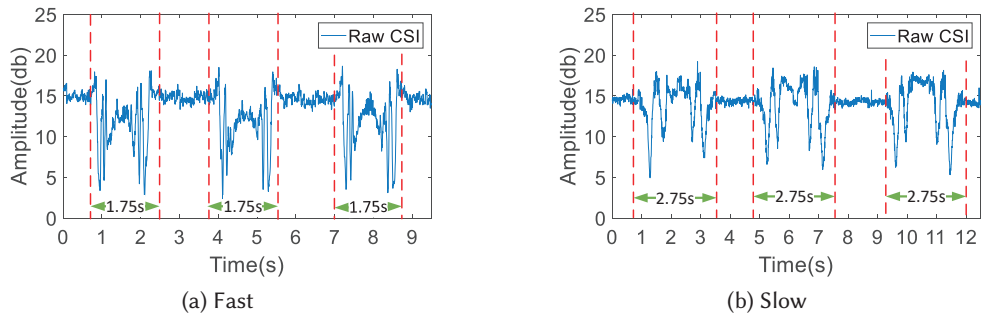


Fig. 22. Accurate time interval obtained for each exercise repetition.

5.4 Assessing if the Exercise Activities are Performed Properly

In this section, we show that the model can guide to assess quality of the activities. We consider three non-standard forms for sit-up: i) the body moves slightly; ii) the body moves to 60 degree; and iii) the body moves close to the ground at 75 degree. Fig. 23 shows the signal patterns of the 3 cases, respectively. The real-life experimental results match the theoretical plots shown in Fig. 17. For case 1, we observe very small signal amplitude variations as the target hardly gets into the FFZ. When the volunteer moves to 60 degree, his back reaches the LoS and blocks half of the FFZ. We can observe clear valleys and the single valley indicates it is not performed properly. If the volunteer moves close to the ground, we observe double valleys, indicating the activity is close to the standard. However, based on the spacing between the valleys, we can still know it is not in a perfect form.

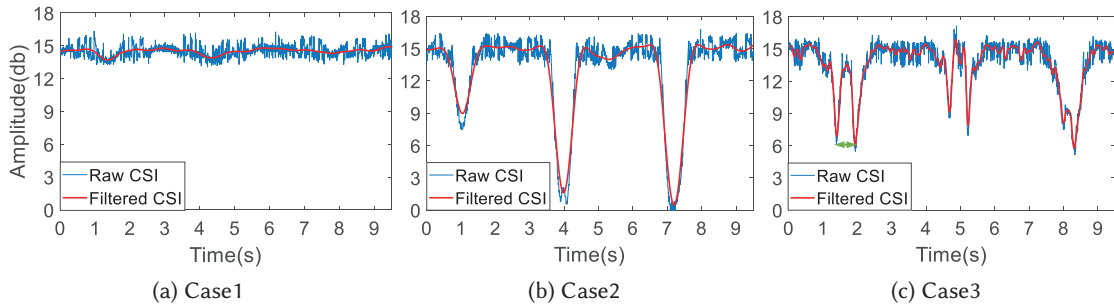


Fig. 23. The signal amplitude patterns obtained with three different non-standard forms of sit-ups.

⁵The system latency is below 0.5 second from the time stamp when the CSI readings are collected to the time stamp when monitoring outputs are obtained.

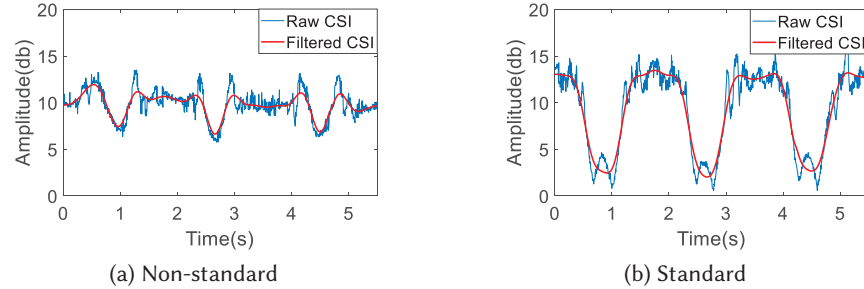


Fig. 24. The amplitude variations are significantly different between non-standard and standard push-ups.

Fig. 24 shows the signal pattern of non-standard push-up compared with the standard one. Here the non-standard (not in a proper form) push-up is defined as a push-up with less than 10 cm body movement while the standard one requires around a 20 cm body movement. We can observe that the non-standard push-up has a much smaller amplitude variation range compared to the standard one. We can accurately identify the non-standard push-ups by checking if the variation range is smaller than the threshold empirically obtained.

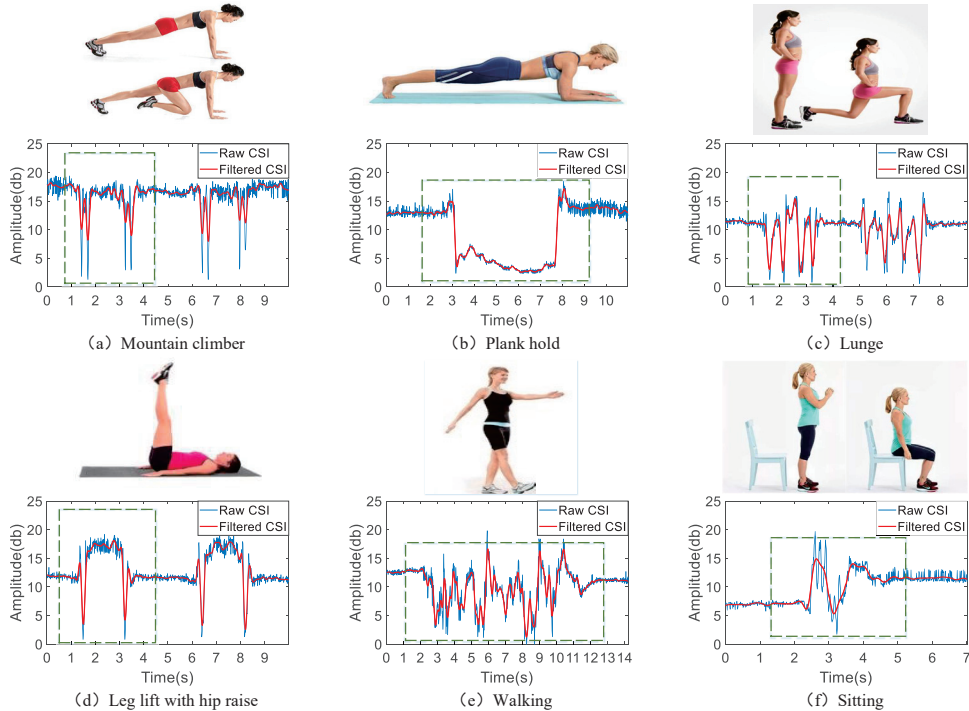


Fig. 25. The signal amplitude patterns for additional 6 activities.

5.5 Extending to More Activities

Now we increase the number of activities to 9 by considering 4 more exercise activities (i.e., mountain climber, plank hold, lunge, leg lift with hip raise), and 2 daily activities (walking and sitting) shown in Fig. 25. We evaluate the system in three different environments, i.e., home, office, and lobby. For each environment, 20 volunteers are asked to perform the 9 activities with 5 repetitions. We obtain a total of 2700 ($3 \times 20 \times 9 \times 5$) activity traces. We employ leave-one-out cross-validation to comprehensively test all the samples in the dataset. To increase the recognition accuracy, we concatenate the CSI amplitude of three antennas as input data. Then we also apply the CNN-based learning network to classify the activities. Fig. 26 shows the confusion matrix of differentiating the 9 activities. The achieved average recognition accuracy is 92.1%.

| Activities | Push-up | Sit-up | Walk-out | Mountain climber | Plank hold | Lunge | Leg lift with hip raise | Walking | Sitting |
|-------------------------|---------|--------|----------|------------------|------------|-------|-------------------------|---------|---------|
| Push-up | 0.96 | 0 | 0.01 | 0.01 | 0 | 0 | 0.01 | 0 | 0.01 |
| Sit-up | 0 | 0.99 | 0.01 | 0 | 0 | 0 | 0 | 0 | 0 |
| Walkout | 0.01 | 0 | 0.86 | 0.01 | 0 | 0.09 | 0 | 0 | 0.03 |
| Mountain climber | 0 | 0 | 0.04 | 0.84 | 0.03 | 0 | 0 | 0.05 | 0.04 |
| Plank hold | 0 | 0 | 0 | 0 | 0.94 | 0 | 0.05 | 0 | 0.01 |
| Lunge | 0 | 0 | 0.04 | 0.01 | 0 | 0.88 | 0 | 0.05 | 0.02 |
| Leg lift with hip raise | 0 | 0 | 0 | 0 | 0.03 | 0 | 0.96 | 0 | 0.01 |
| Walking | 0 | 0 | 0.09 | 0 | 0 | 0 | 0 | 0.91 | 0 |
| Sitting | 0 | 0.01 | 0.02 | 0.01 | 0 | 0.01 | 0 | 0 | 0.95 |

| Activities | Push-up | Sit-up | Walk-out | Mountain climber | Plank hold | Lunge | Leg lift with hip raise | Walking | Sitting |
|-------------------------|---------|--------|----------|------------------|------------|-------|-------------------------|---------|---------|
| Push-up | 0.92 | 0.06 | 0.02 | 0 | 0 | 0 | 0 | 0 | 0 |
| Sit-up | 0.16 | 0.80 | 0.04 | 0 | 0 | 0 | 0 | 0 | 0 |
| Walkout | 0.02 | 0.05 | 0.82 | 0 | 0.02 | 0.09 | 0 | 0 | 0 |
| Mountain climber | 0 | 0.02 | 0 | 0.69 | 0.07 | 0.07 | 0.02 | 0 | 0.13 |
| Plank hold | 0 | 0.05 | 0.09 | 0.09 | 0.68 | 0.09 | 0 | 0 | 0 |
| Lunge | 0 | 0 | 0.08 | 0.02 | 0 | 0.90 | 0 | 0 | 0 |
| Leg lift with hip raise | 0 | 0 | 0 | 0 | 0 | 0 | 0.96 | 0.02 | 0.02 |
| Walking | 0 | 0 | 0 | 0 | 0 | 0 | 0 | 0.84 | 0.16 |
| Sitting | 0 | 0 | 0 | 0.01 | 0 | 0 | 0.02 | 0.09 | 0.88 |

Fig. 26. Confusion matrix of differentiating 9 activities in FFZ. Fig. 27. Confusion matrix of differentiating 9 activities outside FFZ.

5.6 Increasing the Sensing Range

The FFZ is a relatively small region and in this section, we show how to extend the sensing range so the target has a larger movement area and can perform activities in a more flexible manner. First, we do not restrict the target to be within the FFZ. When the target is located outside FFZ, the reflection dominates. The existing work [37] employs Fresnel reflection model for sensing and we can thus utilize Fresnel reflection for sensing outside of FFZ while in the FFZ, we employ the model proposed in this work. We conduct experiments when the target performs activities away from the LoS (outside of FFZ) shown in Fig. 28. We present the confusion matrix of recognition accuracy in Fig. 27. The average recognition accuracy achieved is 83.2%. This accuracy is slightly lower than that when the target is inside FFZ which has larger induced signal variations.

Second, we show that we can further enlarge the sensing range by increasing the LoS distance between the transmitter and receiver. From our experiments, we found that even when the LoS distance is 5 meters, our system can still recognize the preformed activities at high accuracies. We keep the LoS distance as 5m and move the target away from one of the transceivers to the other from 1m to 4m at a step size of 0.5m. The experiment setup is shown in Fig. 29. While the target performs the sit-up activity at different positions, we present the resulted sensing signals in Fig. 30. We find that the sensing signals exhibit similar pattern for the same activity even the target is at different positions. We can thus conclude that the similar patterns ensure the flexibility of target's position inside FFZ.

5.7 Impact of Interference of Surrounding Environment

We study the effect of interference from other persons in the same environment (e.g., the people walking around). We ask people to walk near to the exerciser, and even walk across the LoS to see the impact on our system. We

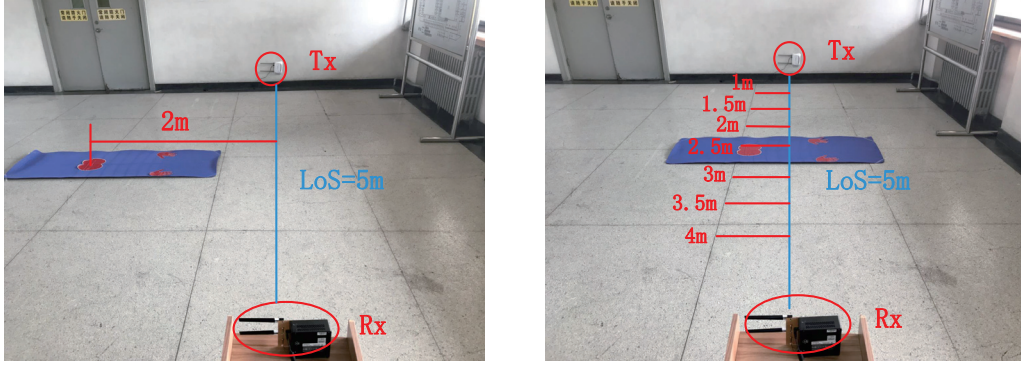


Fig. 28. The target performs activities away from Fig. 29. The target performs activity at different positions in LoS

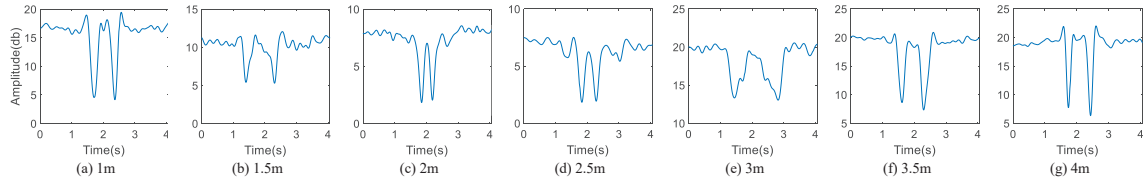


Fig. 30. The signals of sit-up activity at 7 positions

observe that other people's irregular movements around the target cause small scale noise on the signal as shown in Fig. 31a. These small scale signal variations can be easily filtered out with Savitzky-Golay filter shown in Fig. 31b. Thus our system is robust against the interference from other people's movements.

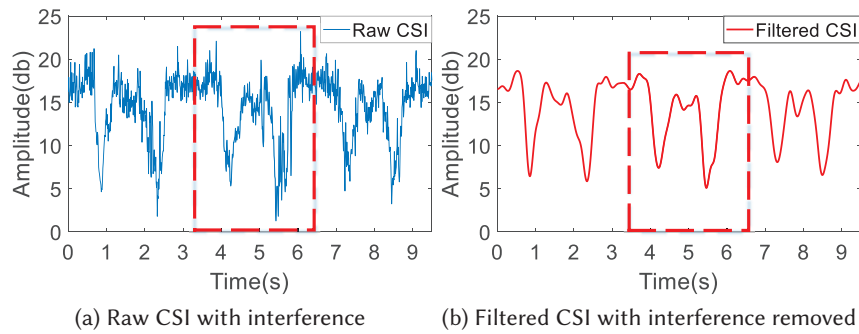


Fig. 31. The impact of interference from other persons.

6 RELATED WORK

This work is broadly related to literature in three areas: exercise monitoring, commodity Wi-Fi based activity recognition systems, and Fresnel model based human sensing.

6.1 Exercise Monitoring

Existing work on physical exercise monitoring include solutions using wearable sensors [6][27] [11][5][2][1] [9], smart phones [13][30], RFID[7] and cameras[57][35]. Consolvo et al. [6] propose to infer the body movement via an on-body sensor to encourage individual's training. Chang et al. [5] track exercises by incorporating an accelerometer into a workout glove. Mortazavi et al. [27] investigate the use of an accelerometer and a gyroscope in smartwatch to count the repetitions of exercises. FitCoach [11] takes one step further by utilizing wearable devices to provide fine-grained tracking of workout and offers exercise review and guidance to improve fitness experience. By using the embedded sensors in smartphone, Hao et al. [13] monitor running by measuring breathing and strides, Pernek et al.[30] manage to detect individual resistance training repetitions. By attaching cheap RFID tags on the dumbbells, Ding et al. [7] propose to recognize various free-weight activities. While all these systems rely on dedicated hardware to be attached to the target for exercise monitoring, it is apparently preferable not to wear anything during exercises. To this end, camera-based systems have long been used to recognize exercises [57], however severe privacy concerns raised and strict lighting requirements limit their wide adoption in home environments. Different from the above solutions, this paper proposes the contactless commodity Wi-Fi based exercise monitoring system, which shows clear advantages in terms of cost and convenience.

6.2 Commodity Wi-Fi Based Activity Recognition Systems

In recent years, with the availability of CSI readings from commodity Wi-Fi devices, significant progresses have been made for device-free sensing, ranging from coarse-grained human tracking [21][31][20][22], human activity recognition [43][39][42][19], to fine-grained vital sign monitoring [24][34][54][29]. Most of these work leverage the signal features and employ machine learning techniques [39][10][17][31][18][8] for classification. RT-Fall [39] automatically segments the fall-like activities from the daily activity CSI stream and accurately detects the fall using a set of selected features. CARM [45] extracts speed-related features from CSI readings and employs Hidden Markov Model(HMM) to recognize several human activities in indoor environment. WiDriver [8] employs BP neural network algorithm to estimate driving actions with CSI amplitude variation data. E-eyes [43] exploits subcarriers of CSI to recognize household activities such as washing dishes and taking a shower. WiFinger [18] further designs a series of signal processing techniques to recognize finger gestures. SEARE [48] proposes to recognize various exercise activity recognition using commercial Wi-Fi devices. While all the activity recognition work relies on the training data samples and selected features, they can not explain the relation between the deployment condition, human activities and the signal patterns. Different from the purely training-based approach, this paper proposes to leverage the Fresnel diffraction model to clearly understand the principle behind sensing effects and guide the activity sensing explicitly.

6.3 Fresnel Zone Model Based Wireless Sensing

Fresnel diffraction model was first introduced for Wi-Fi based device-free localization by Rampa et al. [33] [23] in which they derive a relationship between one's position and the received signal strength. Wang et al. [40] further exploit the Fresnel diffraction model to achieve 0.5 meter localization accuracy using Wi-Fi CSI when the subject is in FFZ. Outside FFZ they employ the path loss model to achieve an average localization accuracy of 1.1 meter. In addition to the above mentioned localization work, Zhang et al. [56] [28] develops the one-side and two-sides Fresnel diffraction model and applied for fine-grained human respiration monitoring.

The first work on human activity sensing leveraging Fresnel reflection model was proposed by Wu et al. [47] and Wang et al. [37]. Both works deal with the case when a subject is outside the FFZ. While Wu et al. [47] utilize the Fresnel reflection model to detect the human walking direction at a median error of less than 10 degrees, Wang et al. [37] apply the Fresnel reflection model for human respiration sensing and reveal that the detectability of human respiration not only depends on the selection of subcarrier, but also one's location and orientation.

Zhang et al. [55] further summarize the properties of Fresnel reflection model for human sensing and derive the sensing limit of Wi-Fi signals. As for the recent work, Wang et al. [38] study the impact of static multipath on the Fresnel zone model and employ the phase difference among multiple subcarriers of the Wi-Fi signal to achieve decimeter-scale indoor localization accuracy, Wu et al. [46] classify the wireless sensing methods into two categories: machine learning-based and model-based solutions. Yang et al. [51] apply the Fresnel reflection model for multiple persons' respiration detection and Xin et al. [50] employ it for human presence estimation. However, all the above human sensing work was only based on the Fresnel reflection model, focusing on the scenarios where the target is outside the FFZ. They did not investigate the scenarios when the target is within the FFZ. Furthermore, none of the work have tried to employ Fresnel diffraction model for coarse-grained human repetitive activity sensing.

Different from all the existing work, we utilize the diffraction effects of RF signals in the FFZ to reveal the reason of unstable performance behind the ML-based methods. We then apply the Fresnel diffraction model to accurately quantify the relationship between the target's movement inside the FFZ and the amplitude change of the received signal. We further develop the Fresnel diffraction based model to guide the repetitive activity sensing and combine it with the ML-based method to demonstrate the effectiveness of the proposed Fresnel model and the model guided ML-based human activity sensing method.

7 CONCLUSION

This paper first investigates the performance of existing machine learning methods used in wireless sensing, and discovers that signal pattern inconsistency induced by human activities makes the sensing system unstable. Motivated by our recent study on Fresnel zone model, we propose a diffraction-based sensing model to establish a quantitative relationship between signal variation and target's activity. We analyze the proposed model theoretically, and apply this model to detect nine diverse activities, including seven body workouts. We build a proof-of-concept prototype to validate and benchmark our system. The proposed model can be applied into many other activities, and can be also used to improve the performance of existing machine learning systems. For our future work, we intend to apply the proposed method to recognize other fine-grained and coarse-grained daily activities.

ACKNOWLEDGMENTS

This work is supported by the National Natural Science Foundation of China (No. 61802373), the National Key Research and Development Plan (No. 2016YFB1001200), the Google European Doctoral Fellowship in Wireless Networking, and the Peking University Information Technology Institute (Tianjin Binhai).

A APPENDIX

Here we present the derivation of the diffraction effect at one side of the target. The signal amplitude at the receiver end due to diffraction can be expressed as [26]

$$F(v) = \frac{1+j}{2} \cdot \int_v^\infty \exp\left(\frac{-j\pi z^2}{2}\right) dz \quad (6)$$

$F(v)$ is known as Fresnel integral. The $\exp\left(\frac{-j\pi z^2}{2}\right)$ is the phase shift for a diffraction path z . Integration with respect to z from v to positive infinity cumulates all diffracted signals at one side of the target. The diffraction gain is given by

$$Gain_{Diff} = 20\log|F(v)| \quad (7)$$

REFERENCES

- [1] 2015. Gymwatch. <https://www.gymwatch.com/>. Online, accessed 10-November-2017.
- [2] 2017. Fitbit. <https://www.fitbit.com/>. Online, accessed 10-November-2017.
- [3] 2017. Pytorch. <https://pytorch.org/>. Online, accessed 20-January-2017.
- [4] Fadel Adib and Dina Katabi. 2013. See Through Walls with Wi-Fi!. In *Proceedings of the ACM SIGCOMM*. ACM, 75–86.
- [5] Keng-Hao Chang, Mike Y. Chen, and John Canny. 2007. Tracking free-weight exercises. In *ACM International Joint Conference on Pervasive and Ubiquitous Computing, UbiComp*. 19–37.
- [6] Sunny Consolvo, David W. McDonald, Tammy Toscos, Mike Y. Chen, Jon Froehlich, Beverly Harrison, Predrag Klasnja, Anthony LaMarca, Louis LeGrand, and Ryan Libby et al. 2008. Activity Sensing in the Wild: A Field Trial of Ubifit Garden. In *Proceedings of ACM CHI*, 1797–1806.
- [7] Han Ding, Jinsong Han, Longfei Shangguan, Wei Xi, Zhiping Jiang, Zheng Yang, Zimu Zhou, Panglong Yang, and JiZhong Zhao. 2017. A Platform for Free-weight Exercise Monitoring with Passive Tags. *IEEE Transactions on Mobile Computing* (2017).
- [8] Shihong Duan, Tianqiang Yu, and Jie He. 2018. WiDriver: Driver Activity Recognition System Based on WiFi CSI. In *International Journal of Wireless Information Networks*. Springer, 146–156.
- [9] Biyi Fang, Nicholas D. Lane, Mi Zhang, Aidan Boran, and Fahim Kawsar. 2016. BodyScan: A Wearable Device for Contact-less Radio-based Sensing of Body-related Activities. In *14th ACM Conference on Mobile Systems, Applications, and Services (MobiSys '16)*. ACM, 4503–4269.
- [10] Chunhai Feng, Sheheryar Arshad, Ruiyun Yu, and Yonghe Liu. 2018. Evaluation and Improvement of Activity Detection Systems with Recurrent Neural Network. In *IEEE International Conference on Communications (ICC)*. IEEE.
- [11] Xiaonan Guo, Jian Liu, and Yingying Chen. 2017. FitCoach: Virtual fitness coach empowered by wearable mobile devices. In *IEEE Conference on Computer Communications, INFOCOM*. IEEE, 1–9.
- [12] Daniel Halperin, Wenjun Hu, Anmol Sheth, and David Wetherall. 2011. Tool release: Gathering 802.11 n traces with channel state information. *ACM SIGCOMM Computer Communication Review* 41, 1 (2011), 53–53.
- [13] Tian Hao, Guoliang Xing, and Gang Zhou. 2015. RunBuddy: A Smartphone System for Running Rhythm Monitoring. In *ACM International Joint Conference on Pervasive and Ubiquitous Computing, UbiComp*. 133–144.
- [14] Wenfeng He, Kaishun Wu, Yongpan Zou, and Zhong Ming. 2015. WiG: WiFi-Based Gesture Recognition System. In *24th International Conference on Computer Communication and Networks*. IEEE.
- [15] Hristo D. Hristov. 1999. *Fresnel Zones in Wireless Links, Zone Plate Lenses and Antennas*. Artech House, Boston, London.
- [16] Hristo D Hristov. 2000. *Fresnel Zones in Wireless Links, Zone Plate Lenses and Antennas*. Artech House, Inc.
- [17] He Li, Kaoru Ota, Mianxiong Dong, and Minyi Guo. 2018. Learning Human Activities through Wi-Fi Channel State Information with Multiple Access Points. In *IEEE Communications Magazine*, Vol. 56. IEEE. Issue 5.
- [18] Hong Li, Wei Yang, Jianxin Wang, Yang Xu, and Liusheng Huang. 2016. WiFinger: talk to your smart devices with finger-grained gesture. In *Proceedings of the 2016 ACM International Joint Conference on Pervasive and Ubiquitous Computing*. ACM, 250–261.
- [19] Shengjie Li, Xiang Li, Qin Lv, Guiyu Tian, and Daqing Zhang. 2018. WiFiFit: Ubiquitous Bodyweight Exercise Monitoring with Commodity Wi-Fi Devices. In *Proceedings of the International Conference on Ubiquitous Intelligence and Computing*. IEEE.
- [20] Xiang Li, Shengjie Li, Daqing Zhang, Jie Xiong, Yasha Wang, and Hong Mei. 2016. Dynamic-MUSIC: accurate device-free indoor localization. In *Proceedings of the International Joint Conference on Pervasive and Ubiquitous Computing, UbiComp '16*. ACM, 196–207.
- [21] Xiang Li, Daqing Zhang, Qin Lv, Jie Xiong, Shengjie Li, Yue Zhang, and Hong Mei. 2016. IndoTrack: Device-Free Indoor Human Tracking with Commodity Wi-Fi. In *Proceedings of the ACM on Interactive, Mobile, Wearable and Ubiquitous Technologies*, Vol. 1. ACM. Issue 2.
- [22] Xiang Li, Daqing Zhang, Jie Xiong, Yue Zhang, Shengjie Li, Yasha Wang, and Hong Mei. 2018. Training-Free Human Vitality Monitoring using Commodity Wi-Fi Devices. In *Proceedings of the ACM on Interactive, Mobile, Wearable and Ubiquitous Technologies (IMWUT)*, Vol. 2. ACM. Issue 3.
- [23] Chen Liu, Dingyi Fang, Zhe Yang, Hongbo Jiang, Xiaojiang Chen, Wei Wang, Tianzhang Xing, and Lin Cai. 2016. RSS distribution-based passive localization and its application in sensor networks. *IEEE Transactions on Wireless Communications* 15, 4 (2016), 2883–2895.
- [24] Xuefeng Liu, Jiannong Cao, Shaojie Tang, Jiaqi Wen, and Peng Guo. 2016. Contactless Respiration Monitoring Via Off-the-Shelf WiFi Devices. *IEEE Transactions on Mobile Computing* 15 (2016), 2466–2479.
- [25] Bishop Christopher M. 1999. In *Pattern Recognition and Machine Learning*. Springer.
- [26] Andreas F. Molisch. 2005. *Wireless Communications*. John Wiley and Sons, Chichester, UK.
- [27] Bobak Jack Mortazavi, Mohammad Pourhomayoun, Gabriel Alsheikh, Nabil Alshurafa, Sunghoon Ivan Lee, and Majid Sarrafzadeh. 2014. Determining the single best axis for exercise repetition recognition and counting on smartwatches. In *11th International Conference on Wearable and Implantable Body Sensor Networks (BSN)*, 33–38.
- [28] Kai Niu, Fusang Zhang, Zhaoxin Chang, and Daqing Zhang. 2018. A Fresnel Diffraction Model Based Human Respiration Detection System Using COTS WiFi Devices. In *Proceedings of the International Symposium on Pervasive and Ubiquitous Computing and Wearable Computers, Ubicomp*. ACM.

- [29] Kai Niu, Fusang Zhang, Jie Xiong, Xiang Li, Enze Yi, and Daqing Zhang. 2018. Boosting fine-grained activity sensing by embracing wireless multipath effects. In *Proceedings of the 14th International Conference on emerging Networking EXperiments and Technologies, CoNEXT*. ACM.
- [30] Igor Pernek, Karin Anna Hummel, and Peter Kokol. 2013. Exercise repetition detection for resistance training based on smartphones. *Personal and ubiquitous computing* 17, 4, 771–782.
- [31] Kun Qian, Chenshu Wu, Zimu Zhou, Yue Zheng, Zheng Yang, and Yunhao Liu. 2017. Inferring motion direction using commodity wi-fi for interactive exergames. In *Proceedings of the 2017 CHI Conference on Human Factors in Computing Systems*. ACM, 1961–1972.
- [32] Pu Qifan, Gupta Sidhant, Gollakota Shyamnath, and Patel Shwetak. 2013. Whole-home gesture recognition using wireless signals. In *Proceedings of the 19th annual international conference on Mobile computing & networking*. ACM, 27–38.
- [33] Vittorio Rampa, Stefano Savazzi, Monica Nicoli, and Michele D’Amico. 2015. Physical Modeling and Performance Bounds for Device-free Localization Systems. *IEEE Signal Processing Letters* 22 (2015), 1864–1868.
- [34] Ruth Ravichandran, Elliot Saba, Ke-Yu Chen, Mayank Goel, Sidhant Gupta, and Shwetak N Patel. 2015. WiBreathe: Estimating respiration rate using wireless signals in natural settings in the home. In *International Conference on Pervasive Computing and Communications (PerCom)*. IEEE, St. Louis, MO, USA.
- [35] Zhou Ren, Junsong Yuan, Jingjing Meng, and Zhengyou Zhang. 2013. Robust part-based hand gesture recognition using kinect sensor. In *IEEE transactions on multimedia*, Vol. 15. IEEE, 1110–1120.
- [36] Ronald W Schafer. 2011. What is a Savitzky-Golay filter? [lecture notes]. *IEEE Signal processing magazine* 28, 4 (2011), 111–117.
- [37] Hao Wang, Daqing Zhang, Junyi Ma, Yasha Wang, Yuxiang Wang, Dan Wu, Tao Gu, and Bing Xie. 2016. Human Respiration Detection with Commodity WiFi Devices: Do User Location and Body Orientation Matter?. In *Proceedings of the International Joint Conference on Pervasive and Ubiquitous Computing, UbiComp ’16*. ACM, 25–36.
- [38] Hao Wang, Daqing Zhang, Kai Niu, Qin Lv, Yuanhuai Liu, Dan Wu, Ruiyang Gao, and Bing Xie. 2017. MFDL: A Multicarrier Fresnel Penetration Model based Device-Free Localization System leveraging Commodity Wi-Fi Cards. *arXiv* (2017).
- [39] Hao Wang, Daqing Zhang, Yasha Wang, Junyi Ma, Yuxiang Wang, and Shengjie Li. 2017. RT-Fall: a real-time and contactless fall detection system with commodity wifi devices. *IEEE Transactions on Mobile Computing* (2017), 511–526.
- [40] Ju Wang, Hongbo Jiang, Jie Xiong, Kyle Jamieson, Xiaojiang Chen, Dingyi Fang, and Binbin Xie. 2016. LiFS: Low Human-Effort, Device-Free Localization with Fine-Grained Subcarrier Information. In *Proceedings of the 22nd Annual International Conference on Mobile Computing and Networking, MobiCom 2016*. ACM, New York City, New York, 243–256.
- [41] Wei Wang, Alex X. Liu, and Muhammad Shahzad. 2016. Gait Recognition Using WiFi Signals. In *Proceedings of the 2016 ACM International Joint Conference on Pervasive and Ubiquitous Computing, UbiComp*. ACM, 363–373.
- [42] Wei Wang, Alex X. Liu, Muhammad Shahzad, Kang Ling, and Sanglu Lu. 2017. Device-free Human Activity Recognition Using Commercial WiFi Devices. *IEEE Journal on Selected Areas in Communications* 35 (2017). Issue 5.
- [43] Yan Wang, Jian Liu, Yingying Chen, Marco Gruteser, Jie Yang, and Hongbo Liu. 2014. E-eyes: device-free location-oriented activity identification using fine-grained wifi signatures. In *Proceedings of the 20th annual international conference on Mobile computing and networking*. ACM, 617–628.
- [44] Yuxi Wang, Kaishun Wu, and Lionel M. Ni. 2017. WiFall: Device-Free Fall Detection by Wireless Networks. *IEEE Transactions on Mobile Computing* 16 (2017), 581–594. Issue 2.
- [45] Wang Wei, Liu Alex X, Shahzad Muhammad, Ling Kang, and Lu Sanglu. 2015. Understanding and modeling of wifi signal based human activity recognition. In *Proceedings of the 21st annual international conference on mobile computing and networking*. ACM, 65–76.
- [46] Dan Wu, Daqing Zhang, Chenren Xu, Hao Wang, and Xiang Li. 2017. Device-Free WiFi Human Sensing: From Pattern-Based to Model-Based Approaches. *IEEE Communications Magazine* 55 (2017).
- [47] Dan Wu, Daqing Zhang, Chenren Xu, Yasha Wang, and Hao Wang. 2016. WiDir: walking direction estimation using wireless signals. In *Proceedings of the International Joint Conference on Pervasive and Ubiquitous Computing, UbiComp ’16*. ACM, 351–362.
- [48] Fu Xiao, Jing Chen, Xiaohui Xie, Linqing Gui, Lijuan Sun, and Ruchuan Wang. 2018. SEARE: A System for Exercise Activity Recognition and Quality Evaluation Based on Green Sensing. In *IEEE Transactions Emerging Topics in Computing*. IEEE.
- [49] Ning Xiao, Panlong Yang, Yubo Yan, Hao Zhou, and Xiang-Yang Li. 2018. Motion-Fi: Recognizing and Counting Repetitive Motions with Passive Wireless Backscattering. In *IEEE International Conference on Computer Communications*. IEEE.
- [50] Tong Xin, Bin Guo, Bin Guo, Pei Wang, Jacqueline Chi Kei Lam, Victor Li, and Zhiwen Yu. 2018. FreeSense: A Robust Approach for Indoor Human Detection Using Wi-Fi Signals. In *Proceedings of the ACM on Interactive, Mobile, Wearable and Ubiquitous Technologies*, Vol. 2. ACM. Issue 3.
- [51] Yanni Yang, Jiannong Cao, Xuefeng Liu, and Kai Xing. 2018. Multi-person Sleeping Respiration Monitoring with COTS WiFi Devices. In *15th International Conference on Mobile Ad Hoc and Sensor Systems (MASS)*. IEEE, 37–45.
- [52] Nan Yu, Wei Wang, Alex X. Liu, and Lingtao Kong. 2018. QGesture: Quantifying Gesture Distance and Direction with WiFi Signals. In *Proceedings of the ACM on Interactive, Mobile, Wearable and Ubiquitous Technologies (IMWUT)*, Vol. 2. ACM. Issue 1.
- [53] Yunze Zeng, Parth H. Pathak, and Prasant Mohapatra. 2016. WiWho: wifi-based person identification in smart spaces. In *15th ACM/IEEE International Conference on Information Processing in Sensor Networks (IPSN)*. IEEE.

- [54] Youwei Zeng, Dan Wu, Ruiyang Gao, Tao Gu, and Daqing Zhang. 2018. FullBreathe: Full Human Respiration Detection Exploiting Complementarity of CSI Phase and Amplitude of WiFi Signals. In *Proceedings of the ACM on Interactive, Mobile, Wearable and Ubiquitous Technologies*. ACM.
- [55] Daqing Zhang, Hao Wang, and Dan Wu. 2017. Toward Centimeter-Scale Human Activity Sensing with Wi-Fi Signals. *IEEE Computer* 50 (2017).
- [56] Fusang Zhang, Daqing Zhang, Jie Xiong, Hao Wang, Kai Niu, Beihong Jin, and Yuxiang Wang. 2018. From Fresnel Diffraction Model to Fine-grained Human Respiration Sensing with Commodity Wi-Fi Devices. In *Proceedings of the ACM on Interactive, Mobile, Wearable and Ubiquitous Technologies*. ACM.
- [57] Wenbing Zhao, Hai Feng, Roanna Lun, Deborah D. Espy, and M. Ann Reinthal. 2014. A Kinect-based rehabilitation exercise monitoring and guidance system. In *Software Engineering and Service Science, 5th IEEE International Conference on*. IEEE, 762–765.

Received August 2018; revised November 2018; accepted January 2019